Available online at www.sciencedirect.com
SCIENCE DIRECT®
Carbohydrate Research 340 (2005) 989–995
Carbohydrate RESEARCH

Effect of the carbohydrate side-chain on the conformation of a glycoconjugate polystyrene in aqueous solution

Isao Wataoka,[a] Kazukiyo Kobayashi[b] and Kanji Kajiwara[a,*]

[a]*Faculty of Textile Science and Technology, Shinshu University, Ueda-shi, Tokoda 3-15-1, 386-8567, Japan*
[b]*Graduate School of Engineering, Nagoya University, Chikusa-ku, Nagoya 464-8603, Japan*

Received 13 September 2004; accepted 24 January 2005

Dedicated to Professor D. A. Brant

Abstract—An oligomaltose-carrying polystyrene ''glycoconjugate polystyrene'' was synthesized by the homopolymerization of 4-vinylbenzylamine oligomaltonic amides, derived from maltose, maltotriose, maltopentaose, and maltoheptaose. The resultant amphiphilic glycoconjugate polystyrenes were dissolved in 0.1 M aqueous urea, and their structures characterized by small-angle X-ray scattering and molecular modeling. ''Glycoconjugate polystyrene'' was found to behave as a ''molecular bottle brush'', composed of a large pseudo-helical polystyrene backbone and carbohydrate brushes. A large pseudo-helical polystyrene backbone is formed by a random sequence of TT, TG, and/or TTGG. The results indicate that the cross-section of a backbone chain with smaller oligosaccharide side-chains is obliged to expand more than that with longer side-chains. Even with rigid hydrophilic pendant oligosaccharide chains, the larger pseudo-helix of the main chain could orient the side-chains so as to envelop the hydrophobic backbone in aqueous solution. Thus the conformation of the main chain is determined not only by the chemical nature of an oligosaccharide chain but also by its length.

Keywords: Glycoconjugate; Small-angle X-ray scattering; Oligosaccharide; Molecular design

1. Introduction

Considerable attention has been paid to the molecular design of biofunctional materials carrying a ligand on synthetic polymers.[1] Those novel materials are expected to have biomedical applications in cell separation, cell culture, as drug delivery agents, and as artificial antigens. Carbohydrates are important candidates as ligands or recognition signals, and thus efforts have been focused on developing a convenient synthetic route[2] for amphiphilic glycoconjugate polymers by arranging hydrophobic polystyrene as a main chain bearing pendant hydrophilic oligosaccharides. Such synthetic glycoconjugate polymers (oligosaccharide-carrying polystyrene derivatives) have indeed been found to function as highly sensitive ligands. Here, highly concentrated multiantennary glyco signals along the hydrophobic main chain enhance the interaction with various types of carbohydrate-binding proteins. The enhancement is also attributed to the presence of the hydrophobic phenyl component, but its active role has not been clearly explained.[3] However, it can be postulated that the activity depends on the chain conformation of a glycoconjugate polymer in water.

The glycoconjugate polystyrene derivative is classified as a type of comb-shaped polymer termed a polymacromonomer, where relatively long branches extend from the backbone chain at a regular intervals. As has been found in most densely grafted polymacromonomers of various combinations, a maltopentaose-carrying polystyrene derivative assumes the shape of a bottle brush in 0.1 M aqueous urea.[4] This molecular bottle brush is

* Corresponding author. Permanent address: Department of Textile Science, Otsuma Women's University, Tokyo, Chiyoda-ku, Sanbancho 12, 102-8357, Japan. Tel.: +81 3 5275 6015; fax: +81 3 3221 7131; e-mail: kajiwara@otsuma.ac.jp

0008-6215/$ - see front matter © 2005 Elsevier Ltd. All rights reserved.
doi:10.1016/j.carres.2005.01.033

composed of a large pseudo-helical polystyrene backbone and maltopentaose brushes. The molecular bottle brush seems to be broken once or twice in segments with no apparent inter-segmental spatial correlation. A large helix of polystyrene is formed by a random sequence of TT, TG, and/or TTGG, because the maltopentaose-carrying polystyrene derivative is atactic and its conformation should, in principle, be a random coil, that is, the backbone-chain conformation is random as a whole, but possesses distinct regions of pseudo-helical parts.

The present work examines the conformation of glycoconjugate polymers bearing pendant malto-oligosaccharides by combining small-angle X-ray scattering (SAXS) and molecular simulation. Particular attention is paid to the effect of side-chain length on the main-chain conformation, which may regulate the physiological function of the side-chains.

2. Experimental

2.1. Materials

4-Vinylbenzyl malto-oligosaccharide amides (VMOA) were synthesized from the respective malto-oligosaccharides lactone by coupling with *p*-vinylbenzylamine, as described elsewhere.[2] The radical homopolymerization of VMOA yields malto-oligosaccharide-carrying polystyrene. Here we prepared four different types of malto-oligosaccharide-carrying polystyrenes by varying the number of maltose residues from 1 to 7. Those are maltose-carrying polystyrene (PVMA), maltotriose-carrying polystyrene (PVMTA), maltopentaose-carrying polystyrene (PVM5A), and maltoheptaose-carrying polystyrene (PVM7A). The structures and sample codes of these malto-oligosaccharide-carrying polystyrenes are summarized in Figure 1.

2.2. X-Ray measurements

The SAXS measurements were carried out with the SAXES[5] installed at BL-10C of Photon Factory, Tsukuba, Japan. The incident X-ray from synchrotron radiation was monochromatized to $\lambda = 1.488$ Å with a double-crystal monochrometer, and then focused onto the position of the detector with a bent focusing mirror. The scattered X-ray was detected by a one-dimensional position-sensitive proportion counter (PSPC) of a effective length 160 mm positioned at a distance of ~1.0 m from the sample holder. The SAXS intensities were accumulated for an appropriate period of time to attain a sufficient signal-to-noise ratio. The exact camera distance was calibrated by using the diffraction peaks of collagen fiber (the long period = 653 Å) at the 6th, 9th, and 11th orders. Data was collected on a CAMAC system controlled by a personal computer system.

The scattered intensities were corrected with respect to the variation of the incident X-ray flux by monitoring the beam with an ionizing chamber placed in front of the thermostated sample holder. The excess scattering intensities were calculated by subtracting the scattering intensities of solvents from those of solutions.

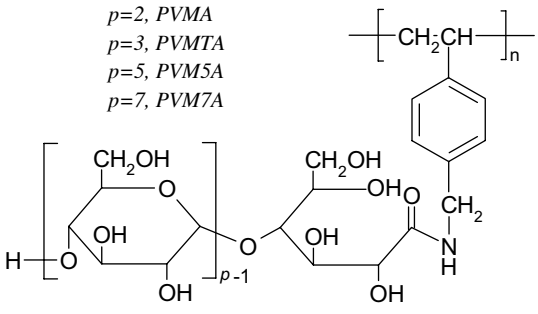

Figure 1. Chemical structures of PVMA, PVMTA, PVM5A, and PVM7A.

2.3. Modeling

A molecular model for maltopentaose-carrying polystyrene (PVM5A) was generated by the use of the program CERIUS2 ver 3.5 (BIOSYM/Molecular Simulations) installed in a Silicon Graphics O2 series workstation. The Universal Force field 1.02 was adapted for energy minimization and molecular dynamics. The molecular mechanics minimization was applied at first to a molecular model constructed manually. The resultant model from the molecular-mechanics minimization was annealed by generating a thermal disturbance. The energy minimization was then performed in a system containing solvent by using a conjugate gradient algorithm, until the root mean square force was less than 0.10 kcal/mol Å, or the number of minimization steps exceeded 3000 in the case of the initial minimization. The molecular-dynamics simulation for annealing was conducted in a constant volume under the conditions identical with those described for energy minimization by molecular mechanics. The temperature of the system was initially fixed at 300 K, then increased to 500 K, and then cooled to 300 K with the temperature increment or decrement of 50 K per 50 steps. One cycle consisted of 50 steps at each temperature from 300 to 500 K and then down to 350 K. The elapsed time for one step corresponds to 0.0010 ps. Thus the total simulation time amounts 2.05 ps.

The conformations of other glycoconjugate polystyrene (PVMA, PVMTA, and PVM7A) were simulated on the basis of that for PVM5A,[4] where the modification was attempted by prefixing the pseudo-helical pitch as described next in order to account for expansion of the pseudo-helix with increase or decrease of the side-chain length.

The intrinsic scattering profile for glycoconjugate polystyrene is proportional to the particle scattering factor, calculated from the atomic coordinates of the simulated novel graft polymer molecule according to the Debye formula Eq. 1.

$$I_{\text{intrinsic}}(q) \approx P(q) = \sum_{i=1}^{n} g_i^2 \phi_i^2(q) + 2\sum_{i=1}^{n-1}\sum_{j=i+1}^{n} g_i g_j \phi_i(q)\phi_j(q) \times \frac{\sin d_{ij}q}{d_{ij}q} \quad (1)$$

where q is the magnitude of the scattering vector given by $(4\pi/\lambda)\sin\theta$ with θ and λ being one half of the scattering angle and the wavelength of the incident X-ray, respectively. g_i Denotes an atomic scattering weight approximately proportional to the atomic number, and d_{ij} is the distance between ith and jth atoms. The form factor for the ith atom $\phi_i(q)$ is assumed to be given by the form factor of a sphere having a radius equivalent to a van der Waals radius of the ith atom as

$$\phi_i(q) = \frac{3[\sin(R_i q) - (R_i q)\cos(R_i q)]}{(R_i q)^3} \quad (2)$$

with R_i being the van der Waals radius of the ith atom. Although the scattering interference term $\sin(d_{ij}q/d_{ij}q)$ in Eq. 1 implies an average over a statistical ensemble, the particle scattering factor is calculated from a single molecule simulated by the molecular dynamics. The system is supposed to be ergodic, the space average should be equivalent to the time average. Since the radius of gyration of a model molecule simulated by the molecular dynamics hardly changes for the last 1000 steps, the conformation of a model molecule is regarded as almost identical to the time-averaged conformation, which in turn is equivalent to that averaged over a statistical ensemble. The consistency of the present procedure has been confirmed for several systems.[6,7] The observed scattering profile should be modified by taking into account the concentration-dependent factor and/or the interference effect.

3. Results and discussion

Figure 2 shows the small-angle X-ray scattering (SAXS) profiles from 2.0 wt. % PVMA, PVMTA, PVM5A, and PVM7A in 0.1 M aqueous urea in the double-logarithmic plots. The effect of side-chain length was observed in the intermediate q range in the scattering profiles. Here, as the side-chain is shorter, the decrease of scattering intensity in the intermediate q range becomes less marked. The SAXS profile reveals a characteristic minimum, depending on the side-chain length at about $0.1\ \text{Å}^{-1} < q < 0.2\ \text{Å}^{-1}$. The position of the scattering

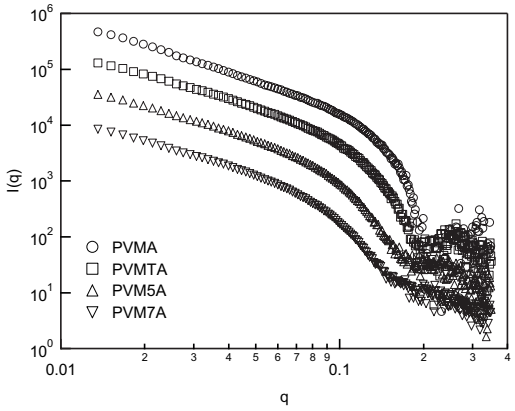

Figure 2. Double logarithmic plot for the glycopolymer solution with PVMA, PVMTA, PVM5A, and PVM7A in 0.1 M aqueous urea in SAXS. The concentrations of each solution are the same (2 wt. %).

minimum seems to be characteristic of the type as well as the length of oligosaccharide side-chains, as a lactose-carrying polystyrene has shown the scattering minimum at $q = 0.23\ \text{Å}^{-1}$.

The scattering from a very long rod can be separated approximately into two independent contributions of the axial factor and the cross-sectional factor as[8]

$$I(q) = L\frac{\pi}{q}\cdot I_c(q) \quad (3)$$

where L is the length of a rod and $I_c(q)$ the scattering from a cross-section. The factor $1/q$ is characteristic of the scattering from a needle with a negligible cross-section. In the same way of the Guinier approximation, the series expansion allows a following approximation under the condition that $qR_{gc} < 1$.[8]

$$I_c(q) \approx \exp(-q^2 R_{gc}^2/2) \quad (4)$$

where R_{gc} is the cross-sectional radius of gyration. R_{gc} is given by $R_{gc}^2 = R^2/2$ for a circular of a homogeneous density, where R denotes a radius of the circular. Eq. 4 indicates that the cross-sectional radius of gyration R_{gc} can be evaluated from the slope in the plots of $\ln(qI(q))$ versus q^2 (the cross-sectional Guinier plot) in an appropriate region of q ($qR_{gc} < 1$). The cross-sectional Guinier plot is shown for a series of malto-oligosaccharide-carrying polystyrenes in Figure 3, and the R_{gc} values evaluated from the scattering profiles are summarized in Table 1. The longer the side-chain of the malto-oligosaccharide-glycopolymer is, the larger is the cross-sectional radius of gyration as qualitatively expected.

The cross-sectional radius of gyration was found to increase as

$$R_{gc} \propto M_{\text{side-chain}}^{0.71} \quad (5)$$

in the polymacromonomer composed of a methylmethacrylate main chain with polystyrene side-chains in

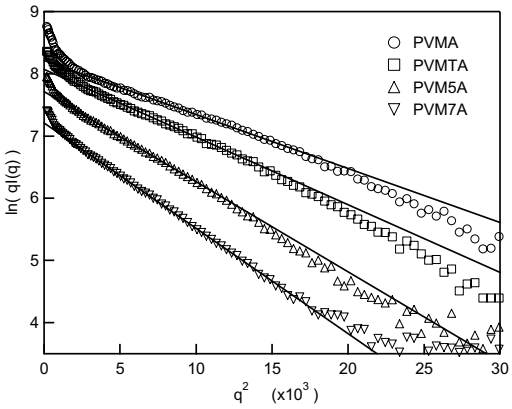

Figure 3. Cross-sectional Guinier plots for PVMA, PVMTA, PVM5A, and PVM7A in 0.1 M aqueous urea (2% by wt). Full lines show the Guinier approximation.

Table 1. Comparison of R_{gc} calculated from experimental profiles and models having same backbone as PVM5A pseudo-helical model[4]

Sample	R_{gc} From experimental (Å)	R_{gc} From model (Å)
PVMA	14.6	10.9
PVMTA	15.6	13.7
PVM5A	17.3	17.8
PVM7A	18.7	20.0

toluene, where $M_{\text{side-chain}}$ denotes the molecular weight of the side-chain.[9] The cross-sectional radius of gyration increases similarly as in Eq. 5 in malto-oligosaccharide-carrying polystyrene as the molecular weight of side-chains increases, but the exponent in Eq. 5 is smaller in this case as evaluated to be 0.20, indicating a major contribution to the cross-sectional radius of gyration from the polystyrene backbone pseudo-helix, owing to the insufficient length of pendant side-chains. The malto-oligomers also assume a pseudo-helical conformation composed of essentially random-coil sequences, so that the characteristic ratio decreases somewhat with increasing degree of polymerization (DP) up to DP $\sim$ 7.[10] The decrease of the characteristic ratio is due to the small increase of the end-to-end distance resulting from the pseudo-helical nature of the malto-oligomer conformation. Since the side-chains are short (at most DP = 7), the change of cross-sectional radius of gyration is predominantly due to that of the backbone pseudo-helix composed of random-coil sequences. The formation of a cylindrical shape is not due to the excluded volume effect of side-chains as in the case of polymacromonomers,[9] but to the amphiphilic characteristics of the glycoconjugate polystyrene composed of hydrophilic side-chains and a hydrophobic backbone. Here the hydrophilic pendant oligosaccharide should cover the hydrophobic backbone polystyrene in water. That is, the glycoconjugate polystyrene is thought to form a kind of a cylindrical molecular micelle.

In order to elucidate the conformational characteristics of a pendant oligosaccharide and a backbone pseudo-helix, molecular models of three malto-oligosaccharide-carrying polystyrenes (maltose-carrying polystyrene PVMA, maltotriose-carrying polystyrene PVMTA, and maltoheptaose-carrying polystyrene PVM7A) were constructed by computer on the base of the skeletal pseudo-helix of maltopentaose-carrying polystyrene PVM5A. Here the skeletal pseudo-helix of PVM5A serves as a standard, as it was proven by observation to yield an almost identical scattering profile.[4] The cross-sectional radii of gyration of those malto-oligosaccharide-carrying polystyrenes are plotted as open circles in Figure 4. Pendant malto-oligosaccharide chains are seen to stick out rigidly from the polystyrene pseudo-helix. A large difference was observed between the experimentally evaluated R_{gc} and the R_{gc} calculated from the molecular models, based on PVM5A with respect to the side-chain length dependence, indicating that the conformational change may take place in the backbone pseudo-helix as the length of pendant malto-oligosaccharide varies. When the side-chain becomes shorter, the backbone helix becomes thicker and shorter, as indicated by the deviation of the calculated R_{gc} from the observed R_{gc}, being larger as in PVMTA and then in PVMA. The cross-section of the skeletal pseudo-helix in the lactose-carrying polystyrene is larger than that of PVM5A.[11] This result suggests that the conformation of the main chain is determined not only by the type of oligosaccharide chain but also by the length of the oligosaccharide chain.

Further modification in each molecular model was attempted by assuming an appropriate fixed length of a cylinder (the end-to-end distance) to take into account the observed tendency of conformational variation. At first a molecular model composed of 32 monomers was artificially constructed, where the end-to-end dis-

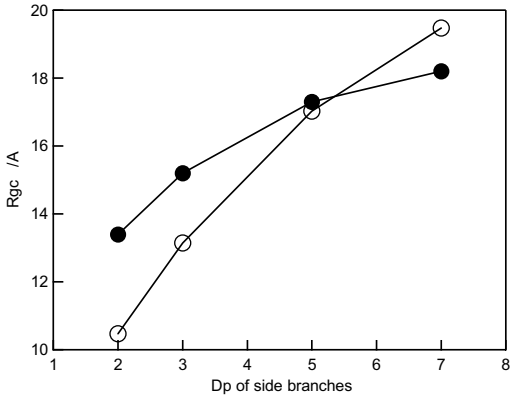

Figure 4. The cross-sectional radius of gyration plots depends on the side-chain length of maltose-carrying glycopolymer. Full circles denote the experimental SAXS data. Open circles represent R_{gcM}, calculated from the molecular model, based on a PVM5A pseudo-helical backbone chain.

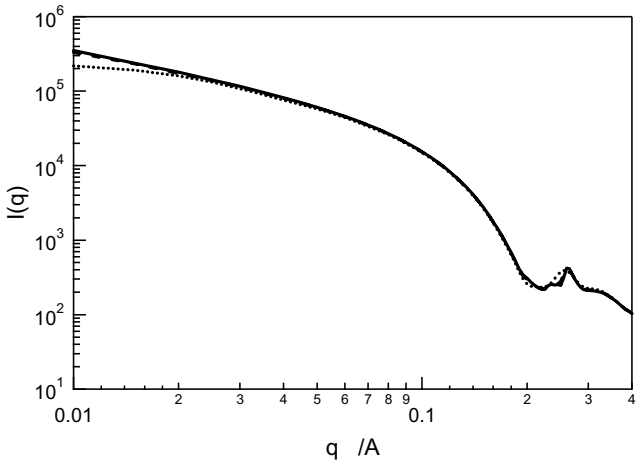

Figure 5. The molecular-weight dependence of the scattering profile calculated for PVMA. No molecular-weight dependence was observed when the DP exceeded 512. The dotted line, broken line, and line represent DP = 256, 512, and 768, respectively.

tance was fixed at an appropriate length. The energy minimization was performed by molecular mechanics (MM) with constrain of the fixed end-to-end distance, and then by the molecular dynamics (MD) under a constant NVT in vacuum at 600 K with Universal Force Field 1.02. In the second step, the end-to-end distance was changed, and the energy-minimization process repeated as just described. Eight molecular models composed of 32 monomers were linked to yield a model of degree of polymerization 256, and the energy minimization was performed with constrain of the fixed end-to-end distance by MM and then by MD as just described. The scattering profile was calculated according to Eqs. 1 and 2. The molecular weight dependence of the scattering profile was examined for PVMA (Fig. 5), where the degree of polymerization was increased up to 768. Since the molecular-weight dependence exhibits a minor effect at $q < 0.02$ Å^{-1}, the degree of polymerization was fixed at 256 for further discussion, and the deviation at smaller q was corrected by taking into account large random aggregates in terms of the Debye–Bueche type scattering function:[12]

$$I_{\text{excess}}(q) \cong \frac{a^3}{(1+a^2q^2)^2} \tag{6}$$

where a denotes a measure for the average size of random aggregates. Thus the total scattering profile is calculated as the sum of a particle-scattering function, Eq. 1, and the excess scattering due to random aggregates Eq. 6 by

$$I_{\text{total}}(q) \approx I_{\text{intrinsic}}(q) + I_{\text{excess}}(q) \tag{7}$$

The results are shown in Figures 6 (PVMA), 7 (PVMTA), 8 (PVM5A), and 9 (PVM7A), and summarized in Table 2. Taking into account the effect of a small amount of aggregation, the fitting is satisfactory, and

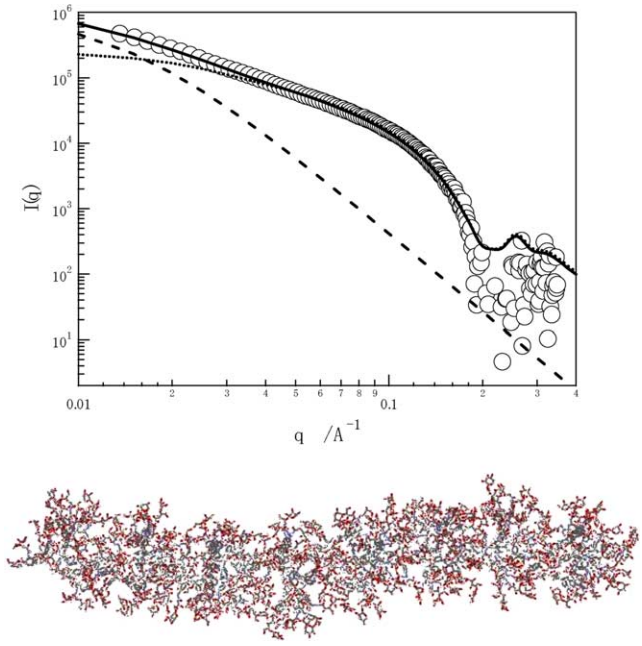

Figure 6. Calculated and observed scattering profile for PVMA. The dotted line and broken line represent $I_{\text{intrinsic}}(q)$ and $I_{\text{excess}}(q)$, respectively. A molecular model is shown at the bottom of the figure.

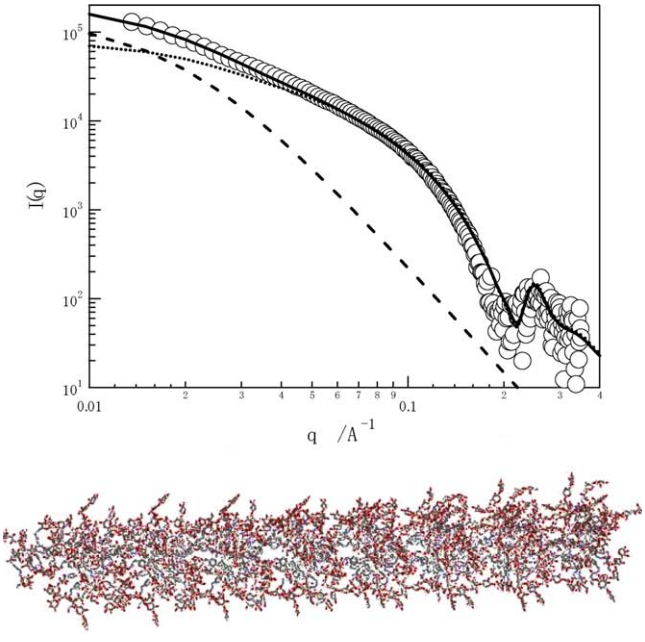

Figure 7. Calculated and observed scattering profile for PVMTA. The dotted line and broken line represent $I_{\text{intrinsic}}(q)$ and $I_{\text{excess}}(q)$, respectively. A molecular model is shown at the bottom of the figure.

the cylindrical shape of simulated molecular models is consistent with the small-angle X-ray results. The results confirm that the pitch of the pseudo-helical conformation of the backbone polystyrene becomes larger with increasing length of the side-chain oligosaccharides, although it is much smaller than that of polystyrene crystals (see Fig. 10). That is, the glycoconjugate forms

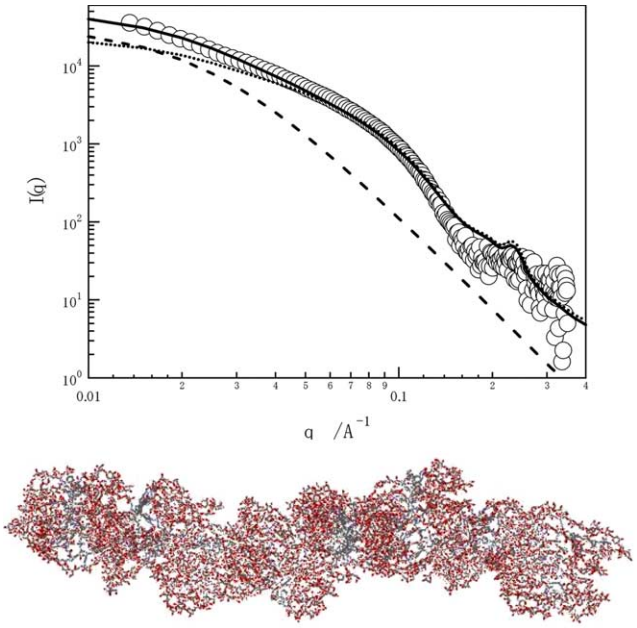

Figure 8. Calculated and observed scattering profile for PVM5A. The dotted line and broken line represent $I_{intrinsic}(q)$ and $I_{excess}(q)$, respectively. A molecular model is shown at the bottom of the figure.

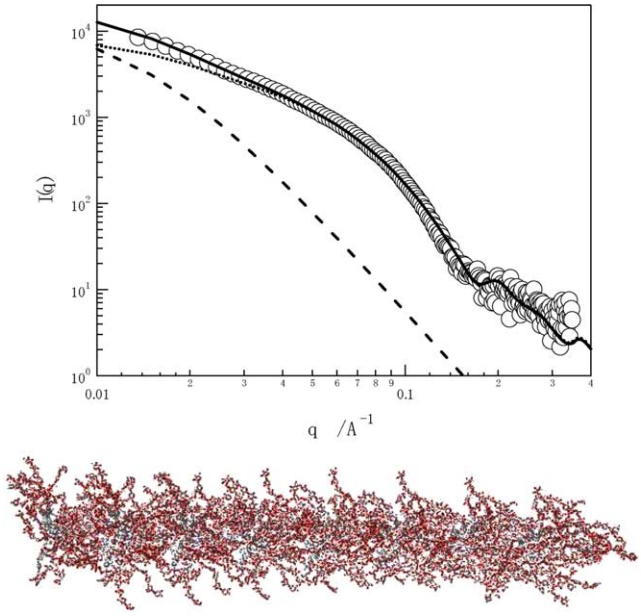

Figure 9. Calculated and observed scattering profile for PVM7A. The dotted line and broken line represent $I_{intrinsic}(q)$ and $I_{excess}(q)$, respectively. A molecular model is shown at the bottom of the figure.

a thick cylindrical shape covered with carbohydrates. Although the end-to-end distance of the malto-oligomer side-chain scarcely increases with increasing DP at the beginning, and not so much as expected from the random-coil conformation,[10] the radius of gyration expands steadily, and the malto-oligomers become longer with increasing DP.[6] In order to accommodate longer

Table 2. The pitch per degree of polymerization in models of fixed length of a cylinder

Sample	Pitch/DP (Å)
PVMA	0.719
PVMTA	0.813
PVM5A	0.903
PVM7A	1.094

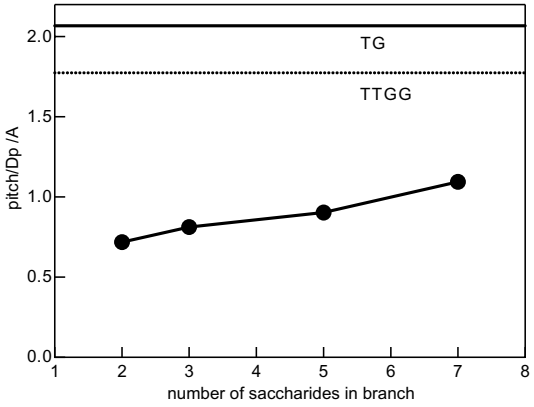

Figure 10. The side-chain length dependence of the pseudo-helical pitch. The pitch of polystyrene helical structure is also shown in the figure.

malto-oligomer side-chains, the main chain is obliged to expand slightly in its axial direction and provide more space for longer side-chains. The backbone chain is almost fully extended in the case of a polymacromonomer, which possesses polymeric side-chains. The change of pitch of pseudo-helical conformation seems to influence the physiological activity of glycoconjugate polystyrene. As observed by the circular dichroism data exhibiting α-helix characteristics,[13] a main-chain conformation specifies the spatial arrangement of optically active oligosaccharide side-chains (covalently linked by an amide linkage to polystyrene backbone).

4. Conclusion

Glycoconjugate polystyrene assumes a pseudo-helical conformation composed of random-coil sequences in aqueous solution, where the oligosaccharide side-chains stick out from the polystyrene backbone. The glycoconjugate polystyrene is optically active, and its whole shape resembles a bottle brush. The diameter of the pseudo-helix of the polystyrene backbone increases with decreasing length of oligosaccharide side-chains in order to cover the entire surface of hydrophobic polystyrene backbone with side-chains. A specific physiological activity (such as cell recognition) of glycoconjugate polystyrene may depend on the length of the oligosaccharide side-chains, which determines the spatial arrangement of biofunctional carbohydrates.

Acknowledgements

This work was performed under approval by the Photon Factory Advisory Committee (proposal No. 94G293, 97G139). We thank Professor H. Urakawa for his assistance in the SAXS measurements. Financial support was from a Grant-in-Aid for Scientific Research on Priority Areas from the Ministry of Education, Culture, Sports and Science, Japan.

References

1. Kobayashi, K.; Kobayashi, A.; Akaike, T. *Methods Enzymol.* **1994**, *247*, 409–418.
2. Kobayashi, K.; Sumitomo, H.; Ina, Y. *Polym. J.* **1985**, *17*, 567–575.
3. Kobayashi, K.; Tsuchida, A.; Usui, T.; Akaike, T. *Macromolecules* **1997**, *30*, 2016–2020.
4. Wataoka, I.; Urakawa, H.; Kobayashi, K.; Akaike, T.; Schmidt, M.; Kajiwara, K. *Macromolecules* **1999**, *32*, 1816–1821.
5. Ueki, T.; Hiragi, Y.; Izumi, Y.; Kataoka, M.; Muroga, Y.; Matsushita, T.; Amemiya, Y. *Photon Factory Activity Rep.* **1983**, *1*, V5, V29, V170.
6. Shimada, J.; Kaneko, H.; Takaha, T.; Kitamura, S.; Kajiwara, K. *J. Phys. Chem.* **2000**, *104*, 2136–2147.
7. Kajiwara, K.; Miyamoto, T. In *Polysaccharides: Structural Diversity and Functional Versatility*; 2nd ed., Dumitriu, S., Ed.; Marcel Dekker: New York, 2004; pp 1–40.
8. See, for example, *Small Angle X-ray Scattering*; Glatter, O., Kratky, O., Eds.; Academic: London, 1982.
9. Wintermantel, M.; Gerle, M.; Fischer, K.; Schmidt, M.; Wataoka, I.; Urakawa, H.; Kajiwara, K.; Tsukahara, Y. *Macromolecules* **1996**, *29*, 978–983.
10. Jordan, R. C.; Brant, D. A.; Cesaro, A. *Biopolymers* **1978**, *17*, 2617–2632.
11. Wataoka, I.; Urakawa, H.; Kobayashi, K.; Ohno, K.; Fukuda, T.; Akaike, T.; Kajiwara, K. *Polym. J.* **1999**, *31*, 590–594.
12. Debye, P.; Bueche, A. M. *J. Appl. Phys.* **1949**, *20*, 518–523.
13. Shimojo, S.; Cho, C. S.; Park, I. K.; Kunou, M. Goto, M.; Akaike, T. *Carbohydr. Res.* **2003**, *338*, 2129–2133.